Studies of Diffusional Release of a Dispersed Solute from Polymeric Matrixes by Finite Element Method

X. Y. WU* AND Y. ZHOU

Contribution from *Department of Pharmaceutical Sciences, Faculty of Pharmacy, University of Toronto, Toronto, Ontario, Canada M5S 2S2.*

Received November 9, 1998. Final revised manuscript received April 13, 1999.
Accepted for publication July 30, 1999.

Abstract □ This paper presents systematic analyses by the finite element method of release kinetics of a dispersed solute from various matrixes (i.e., slab, sphere, cylinder, and convex tablet), with or without boundary-layer resistance, into a finite or an infinite external volume. In the case of sink conditions, the numerical results agree well with the existing analytical solutions. For the problems of solute release into a finite external volume, where the analytical solutions are not available, this work has provided numerical solutions of the differential equations describing the release kinetics, moving boundaries, and concentration profiles. This work has also revealed the dependence of release kinetics on the initial solute loading, the external volume, and the boundary-layer thickness. The method presented here can describe the entire process of diffusional release before and after the dispersed solute has been dissolved without the pseudo steady-state assumption and it is applicable to both small and large ratio of initial solute loading to the solute solubility in the matrix.

Introduction

The kinetics of diffusional release of a dispersed solute, i.e., the initial solute loading (A) is higher than the solute solubility in the matrix (C_s), has been a subject of practical importance in controlled drug delivery. Drug delivery systems such as pharmaceutical solid dosage forms often contain dispersed biologically active agents, which makes it difficult to solve the differential equations and thus predict the release kinetics of the agents because of a moving boundary of the dispersed solute. The task becomes more complicated when the solute is released from a multidimensional dosage form, such as a convex tablet, with boundary-layer resistance into a finite external medium. So far, no analytical solution has been made available for investigation of such a complex system.

In the past decades, a number of mathematical models have been developed to describe the release kinetics of dispersed solutes[1−17] mainly for one-dimensional release except for ref 6. The majority of the models postulate infinite well-agitated sink, that is, no boundary layer resistance and no solute accumulation in the release medium due to the mathematical complication. A few groups have considered boundary-layer resistance under the sink condition[2,3,11] and in a finite external medium.[12] It must be noted that the analytical or semianalytical solutions of the above models are only applicable to the release process up to the time, t^*, for all the dispersed solute to dissolve,[3,4,17] except for those with a pseudo steady-state assumption.[1,2,6,10,12] This is because the concentration distribution in the matrix at t^* is nonuniform and unknown ahead of time. For a matrix with a small A/C_s ratio, a considerable amount of dissolved solute remains in the matrix at time t^*, whose contribution to the release kinetics is not described by the models without a pseudo steady-state assumption.[3,4,17] To overcome the difficulty, a linear distribution is assumed in the pseudo steady-state approach.[1,2,6,10,12] This approach has been applied extensively for $A \gg C_s$ and sink conditions or near-sink conditions with success especially for planar geometry.[3,4,16] Nevertheless, when the A/C_s ratio is small, for example, when $A/C_s = 2$ or approaches 1, the real concentration distribution deviates from the linear one noticeably. As a consequence, prediction by the pseudo steady-state approach becomes less accurate.[3,4]

In practice, drug release from a dosage form into a finite volume of surrounding medium is often found. In this case, the release rate may be reduced as a consequence of drug accumulation in the medium, deviating from the prediction by the models for sink conditions. Such an effect can be expected when the drug removal from the medium is slow or the drug solubility in the medium is minimal, typified by drug release in the lower gastrointestinal tract where liquid content and absorption rate are relatively low, or from an implant or an insert into a confined cavity such as solid tumors and root canals. Therefore, prediction of release kinetics for these dosage forms in a finite external volume is of more practical importance than that for sink conditions, although both may be governed by the same release mechanism.

The analytical solutions for solute release into a finite volume can be found for one-dimensional release from slab, sphere, and cylinder with a loading, $A \leq C_s$. Nevertheless, there is no analytical solution available for release kinetics of sphere, cylinder, and convex tablet with a boundary layer and $A > C_s$ in a finite volume, except that for a sphere with assumptions of pseudo steady-state and boundary-layer thickness much smaller than the radius of the sphere.[12] This is perhaps because of the above-mentioned difficulty involving the moving boundary of the solute, time-dependent boundary condition, and nonuniform solute concentration in the matrix at t^*. Therefore, numerical methods must be applied in order to solve the differential equations for such systems.

The objective of this work is to study the kinetics of the entire process of diffusional release of an initially dispersed solute from polymeric matrixes into a finite external volume with or without the boundary-layer effect. The finite element method, a computer-aided numerical approach, is employed to solve the differential equations. The release profiles for matrixes of various shapes (i.e., slab, sphere, cylinder, and convex tablet) are presented for different A/C_s ratios and various external volumes ranging from infinite to a small liquid/matrix volume ratio. The evolution of solute concentration in these matrixes and the

* Corresponding author. Tel. (416)978-5272; fax: (416)978-8511; e-mail: xywu@phm.utoronto.ca.

10.1021/js9804361 CCC: $18.00
Published on Web 09/08/1999

effect of boundary-layer resistance are discussed based on the numerical results.

Theoretical Background

It is assumed that dissolution of a dispersed solute is rapid compared with the subsequent depletion of the solute by diffusion. The process of diffusional release of a dispersed solute from a matrix can be physically visualized[18] as a process of solute extraction, i.e., the solution of the dispersed solute followed by the diffusion of the dissolved solute. Initially, the dispersed solute is dissolved and diffuses out from the surface layer; after a certain time, the solute concentration in the surface layer is reduced to the saturated level (C_s), and the extraction of the solute in the next layer is initiated. Between the just-extracted layer and the next layer, there exists a sharp concentration gradient, i.e., the moving boundary of the dispersed solute, and the concentration difference between the two layers is $A - C_s$. The boundary will move inward layer by layer continuously until all the dispersed solute is dissolved.

Since the process is diffusion-controlled, the governing equation of the diffusion is held for the whole process no matter whether the solute is dispersed or dissolved. The general expression of the governing equation for a problem of three-dimensional and homogeneous material with boundary layer resistance in a well-mixed finite external medium is given as follows,

$$\frac{\partial C_i}{\partial t} = \nabla\cdot(D_i \nabla C_i) \qquad i = 1, 2 \tag{1}$$

where ∇ is the differential operator, the suffixes 1 and 2 denote the polymeric matrix and the boundary layer, D_i and C_i are the diffusion coefficient (cm^2/s) and solute concentration (g/cm^3) in these two domains, respectively. Definition of these domains and relevant boundaries for an arbitrary geometry is illustrated in the following schematic diagram:

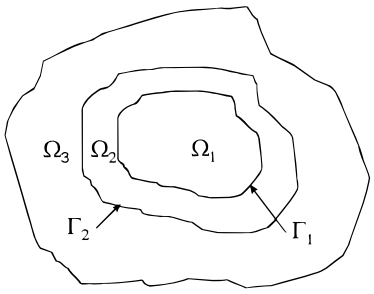

The corresponding initial and boundary conditions are

$$C_1 = A, \text{ in } \Omega_1, t = 0 \tag{2}$$

$$C_2 = C_3 = 0, \text{ in } \Omega_2 \text{ and } \Omega_3, t = 0 \tag{3}$$

$$D_1\frac{\partial C_1}{\partial n} = D_2\frac{\partial C_2}{\partial n}, \text{ on } \Gamma_1, t > 0 \tag{4}$$

$$C_1 = KC_2, \text{ on } \Gamma_1, t > 0 \tag{5}$$

$$(A - C_s)\frac{d\xi}{dt} = D_1|\nabla C_1|, \text{ on } \xi(t), 0 < t < t^* \tag{6}$$

$$C_1 = C_s, \text{ on } \xi(t), 0 < t \le t^* \tag{7}$$

$$V\frac{\partial C_3}{\partial t} = D_2\frac{\partial C_2}{\partial n}S_2, \text{ on } \Gamma_2, t > 0 \tag{8}$$

where A is the initial solute loading (g/cm^3), K is the partition coefficient, $\xi(t)$ is the moving boundary, Ω_1, Ω_2, and Ω_3 are the domains of the matrix, boundary layer, and the finite external medium, respectively. Γ_1 and Γ_2 denote the boundaries of Ω_1 and Ω_2, S_2 is the area of the interface between Ω_2 and Ω_3. V is the volume of the finite external medium, and t^* is the time for all the dispersed solute to dissolve. In eqs 4 and 8,

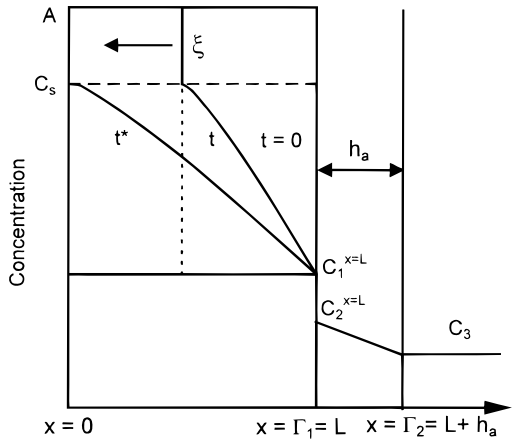

Figure 1—Schematic diagram of moving boundary, boundary layer, and concentration profile for a one-dimensional slab, sphere, and cylinder, where L denotes either the half-thickness of a slab, or radius of a sphere or a cylinder; $x = 0$ stands for the midplane or the center of the matrixes.

$$\frac{\partial C}{\partial n} = n_x\frac{\partial C}{\partial x} + n_y\frac{\partial C}{\partial y} + n_z\frac{\partial C}{\partial z} \tag{9}$$

where n_x, n_y, and n_z are the directional cosines of the outward normal n to the closed boundary Γ_i.

For a sink condition, the boundary condition described by eq 8 is replaced by eq 10,

$$C_3 = 0 \qquad \text{on } \Gamma_2 \qquad t \ge 0 \tag{10}$$

For the matrixes with one-dimensional release such as a sphere, an infinite slab or an infinitely long cylinder, the above equations can be simplified to conventional presentations[2–4] as illustrated in Figure 1, where ξ is the moving boundary of the dispersed solute, x is the distance, L is the half thickness of a slab or the radius of a sphere or a cylinder, h_a is the thickness of the boundary layer, $C_1^{x=L}$ is the concentration in the matrix at x = L, $C_2^{x=L}$ is the concentration in the boundary layer at $x = L$, C_3 is the concentration in the bulk solution. For a system with no boundary-layer resistance, $C_2 = C_3$; a system in a sink with boundary layer, $C_3 = 0$; and a system in a sink without boundary layer, $C_2^{x=L} = C_2 = C_3 = 0$.

As aforementioned, the whole release process is diffusion-controlled. Therefore, the computational procedures of the finite element method developed in the previous work[19–22] for dissolved solute are still applicable to the release of dispersed solute except that eqs 6 and 7 need to be incorporated into the computation. Mathematically these equations represent the instantaneous mass balance at the diffusion moving front. Physically they can be viewed as that, in order for the diffusion front to move a distance δx in a time δt per unit area perpendicular to x, an excess amount of solute, $(A - C_s)\delta x$, must be removed by diffusion. Based on this interpretation, the computational procedures were correspondingly modified to incorporate eqs 6 and 7. The whole matrix domain was divided into many thin layers. The diffusion was initiated from the most outer layer. The solute concentration in the current thin layer was examined at very small time intervals using an iteration checking subroutine. Once the excess amount of

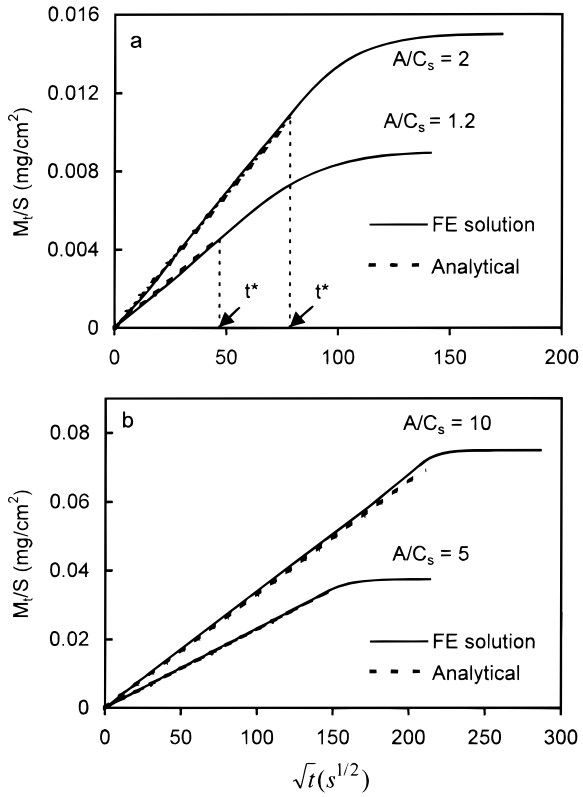

Figure 2—Cumulative amount of a dispersed solute released per unit surface area from a slab into a perfect sink ($L = 0.1$ cm, $D_1 = 1 \times 10^{-6}$ cm^2/s). (a) $A/C_s = 1.2$ and 2; (b) $A/C_s = 5$ and 10.

solute, $(A - C_s)\delta x$, had been depleted, i.e., $C_1 = C_s$ in the current layer, the solute diffusion in the next thin layer was allowed. Otherwise the iteration continued until the saturation level was reached. The amount of solute released (M_t) at time t was obtained by subtracting the amount of solute remained in the matrix from the initial amount of solute. The remaining was calculated by multiplying the solute concentration in each finite element at time t by the volume of the element.

Results and Discussion

To verify the computational procedures and results, release profiles of a dispersed solute from a one-dimensional slab, sphere, and cylinder into a sink were first calculated and compared with the available analytical solutions. Release kinetics for three basic geometries and convex tablet in different external volumes and its dependence on the boundary-layer resistance and initial solute concentration were then studied.

One-Dimensional Release and Verification—*(a) Slab*—Figure 2 depicts the amount of the drug released per unit surface area of a slab as a function of square root of time. Evidently, the results of this work agree well with the analytical solution by Paul and McSpadden[3] at earlier stage, i.e., $t \leq t^*$. At a later stage, i.e., $t > t^*$, the analytical solution is no longer applicable, whereas the finite element solution continuously describes the rest of the release process. When the A/C_s ratio is large, e.g., $A/C_s = 10$ or 5, the analytical solution may be extended to $t > t^*$ with an acceptable error, as only a small portion of the solute remains in the matrix. Nevertheless, the error can be significant when the A/C_s ratio is small. As will be discussed in section d), there is still about 50% of the solute unreleased at t^* for $A/C_s = 1.2$ and 28% for $A/C_s = 2$. This implies that up to 50% of the solute is released by a different mechanism (i.e., no moving boundary). The release kinetics of this portion of the solute cannot be described by the analytical solution. Therefore, the straight line predicted by the model was linearly extrapolated and linked with the horizontal line of 100% release.[3] The experimental data showed that the release profile is a asymptotic curve approaching to the 100% line,[3] especially for small A/C_s ratios. This experimental observation is predicted by the numerical solutions of this work (Figure 2a).

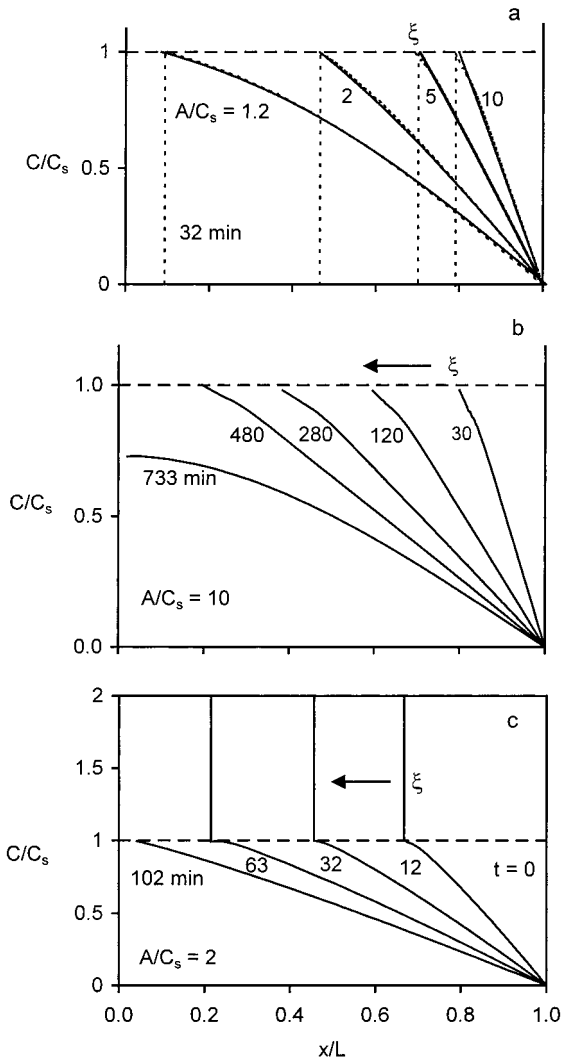

Figure 3—Moving boundary of a solid solute and concentration profile for a sphere with various A/C_s ratios in a perfect sink ($L = 0.1$ cm, $D_1 = 1 \times 10^{-6}$ cm^2/s). (a) Time = 32 min, $A/C_s = 1.2$, 2, 5, and 10, (- - - -) Paul and McSpadeen,[3] (—) FEM; (b and c) $A/C_s = 10$ and 2, respectively, at various time intervals.

Figure 3a compares the concentration distribution of a solute in the matrix for different A/C_s ratios at the same time (32 min). A good agreement between this work and the analytical solution[3] is evidenced. Apparently, the smaller the A/C_s ratio, the more advanced the moving boundary of the dispersed solute, due to smaller excess amount of solute to be removed by diffusion. Figures 3b and 3c illustrate the progress of the moving boundary and concentration distribution at different times for $A/C_s = 10$ and 2, respectively. It is noticed that more linear distribution curves are obtained at $A/C_s = 10$ than those at $A/C_s = 2$, supporting Higuchi's pseudo steady-state assumption for $A \gg C_s$.[1]

The amount of solute released into a well-mixed finite medium with the effective volume ratio, $\lambda = V/(V_1K) = 5$,

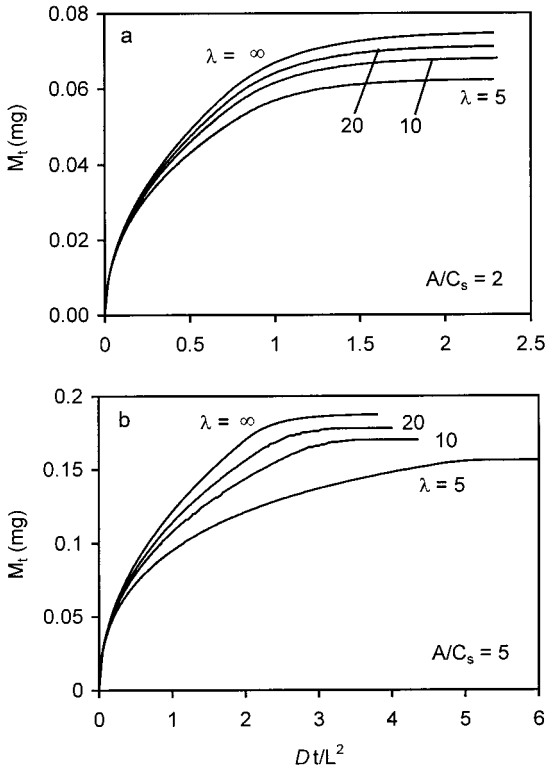

Figure 4—Influence of effective volume ratio on the amount of solute released from a slab into a well-mixed liquid of finite volume ($L = 0.1$ cm, $D_1 = 1 \times 10^{-6}$ cm^2/s, $K = 1$). (a) $A/C_s = 2$ and (b) $A/C_s = 5$. The 100% solute released is indicated by the plateau of the release curve for $\lambda = \infty$.

10, 20, and ∞, is plotted against D_t/L^2 in Figure 4 for (a) $A/C_s = 2$ and (b) $A/C_s = 5$, where $K = 1$, V and V_1 are the volume of the liquid and the matrix, respectively. The influence of the effective volume ratio on the release rate is consistent with previous analytical and experimental results.[19,21] It is shown that the release rate and the final amount of the solute decrease with the decrease in λ value. Given a fixed partition coefficient, this observation can be attributed to quicker concentration build-up and consequently higher diffusional resistance in a smaller volume. Note that at $A/C_s = 5$, the influence of λ becomes more profound as indicated by larger differences among the curves in Figure 4b compared to those in Figure 4a. In addition, more abrupt change in the curves before reaching the plateau is observed for $A/C_s = 5$. This is an indication of inhibition of release by the saturation of the solute in the liquid at higher A/C_s ratios. The analysis can also be carried out in the same way for the effect of K value and for the solute released into a poorly mixed external finite volume.[20]

(b) Sphere—Figure 5 shows the amount of the released solute versus D_t/L^2 for a spherical matrix in a perfect sink by this work compared with the approximate analytical solutions derived by Lee[4] and by Baker and Lonsdale.[5] It is depicted that this work agrees well with Lee's solution at $A/C_s = 2$ and with Baker and Lonsdale at $A/C_s = 5$ and 10. It should be pointed out that the latter, with pseudo steady-state assumption, is restricted to A/C_s ratio > 3 or 4,[16] while the former is suitable for small A/C_s ratios and $t \leq t^*$. In contrast, the numerical method presented in this work, with no restriction, can predict the entire release process for various A/C_s ratios.

As delineated by Figure 6, the progress of the moving boundary is much faster in spheres than that in slabs. Interestingly, due to the spherical geometry, the concentration profiles are considerably nonlinear compared with that in the slab even at a high A/C_s ratio. The distribution curve

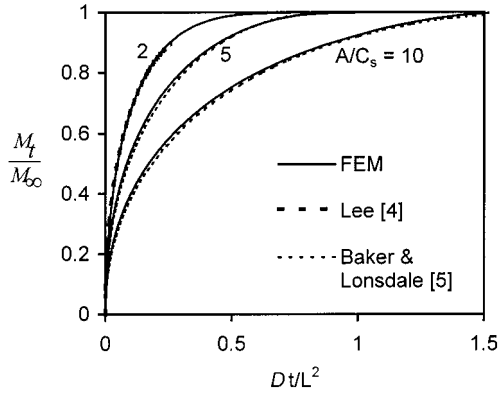

Figure 5—Fractional release of a dispersed solute from a sphere into a perfect sink ($L = 0.1$ cm, $D_1 = 1 \times 10^{-6}$ cm^2/s). Comparison of finite element solution with semianalytical solution from Lee[4] and solution from Baker and Lonsdale with pseudo steady-state assumption.[5]

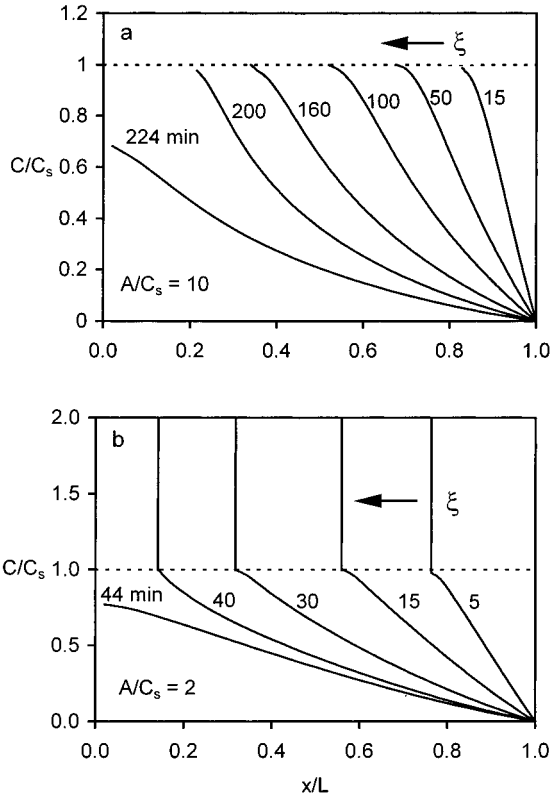

Figure 6—Moving boundary of a solid solute and concentration profile for a sphere in a perfect sink ($L = 0.1$ cm, $D_1 = 1 \times 10^{-6}$ cm^2/s). (a) $A/C_s = 10$ and (b) $A/C_s = 2$.

is gradually changed from convex to concave due to the relative change rate between the surface area of the dispersed solute core and the diffusional distance which is the distance from the moving boundary to the matrix surface.

The amount of the solute released into a well-mixed finite volume with the effective volume ratio, $\lambda = 5$, 10, 20, and the sink condition is presented in Figure 7. The dependence of the release kinetics on the volume ratio and initial loading is similar to that in planar geometry.

(c) Cylinder—The only available analytical solutions for the cylindrical geometry were developed by Crank[23] and Roseman and Higuchi.[2] The former is applicable to $A/C_s \leq 1$ and the latter is an approximate solution and only suitable for $A \gg C_s$ under the sink condition. No analytical solution is available for a cylindrical matrix with a small A/C_s ratio ($A > C_s$) in either a perfect sink or a finite

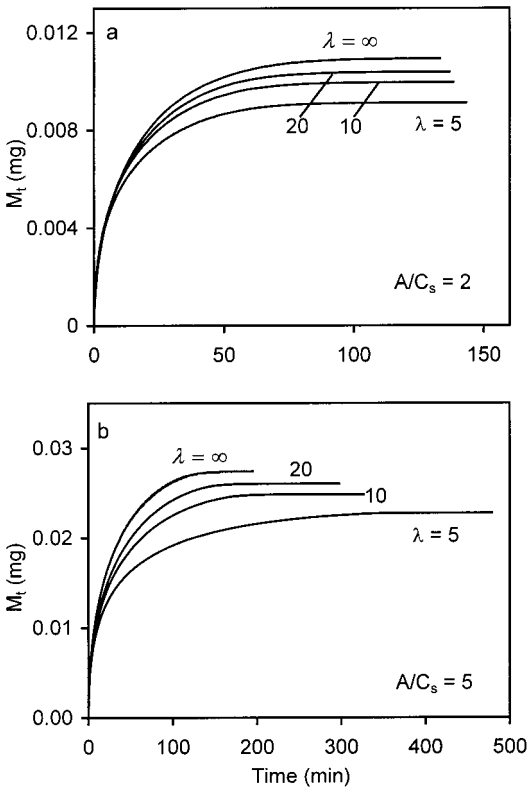

Figure 7—Influence of effective volume ratio on the amount of solute released from a sphere into a well-mixed liquid of finite volume ($L = 0.1$ cm, $D_1 = 1 \times 10^{-6}$ cm^2/s, $K = 1$). (a) $A/C_s = 2$ and (b) $A/C_s = 5$. The 100% solute released is indicated by the plateau of the release curve for $\lambda = \infty$.

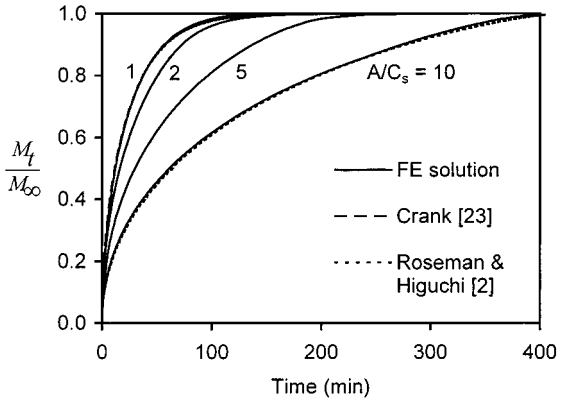

Figure 8—Fractional release of a dispersed solute from a cylinder into a perfect sink ($L = 0.1$ cm, $D_1 = 1 \times 10^{-6}$ cm^2/s, $A/C_s = 1$, 2, 5, and 10).

volume, and there is little knowledge of the concentration distribution in the cylinder. Therefore, Crank's and Roseman and Higuchi's solutions are used here as bounding cases to verify the finite element results. As shown in Figure 8, a very convincing agreement has been obtained between the finite element solutions and the analytical ones in both lower ($A/C_s = 1$) and upper ($A/C_s = 10$) bounding cases. For the A/C_s ratios between these two extremes, where the analytical solutions are not applicable, the solutions of this work have filled the gap. It is expected that the present numerical approach can provide reliable solutions for a broad range of A/C_s ratios from $A/C_s \leq 1$ to $A \gg C_s$.

The progress of the moving front versus time and the concentration distribution in the cylinder for $A/C_s = 2$ and 10 are presented in Figure 9. By comparison of the concentration profiles of slab, sphere, and cylinder, i.e., Figures 3b, 6a, and 9a, some interesting features are

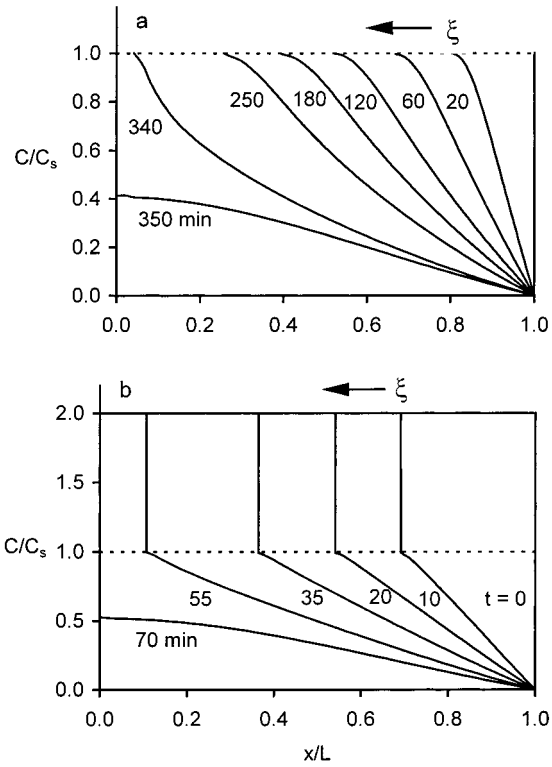

Figure 9—Moving boundary of a solid solute and concentration profile for a cylinder in a perfect sink ($L = 0.1$ cm, $D_1 = 1 \times 10^{-6}$ cm^2/s). (a) $A/C_s = 10$ and (b) $A/C_s = 2$.

noticed. In the slab, the concentration distribution is near linear and always convex. The concentration profile becomes nonlinear and is gradually changed from convex to concave with time in the cylinder. The more nonlinear concentration profile is observed in the sphere with a faster change from convex to concave than in the cylinder. This phenomenon can be ascribed to the inherent difference in the geometry. For diffusional release from matrixes with a dispersed solute, the concentration distribution depends on the relative change rate of the surface area of the solid core and the diffusional distance. The former determines the supply of the solute for diffusion, and the latter determines the time for the solute to leave the matrix. Although surface area and diffusional distance are functions of the moving front in all three geometries, the dependence of the area on the distance is zero for slab, linear for cylinder, and quadratic for sphere. In other words, the relative rate of reduction in the surface area of the undissolved core is the highest in the sphere and the lowest in the slab. Consequently, the change from convex to concave occurs more dramatically in the sphere due to insufficient solute supply for diffusion.

Figure 10 presents the amount of the drug released into different external volumes for cylinders with (a) $A/C_s = 2$ and (b) $A/C_s = 5$. The figures reveal that the influence of volume ratio on the release kinetics for cylinder is similar to that for planar and spherical geometries (Figures 4 and 7). These results are particularly useful for prediction of in vivo release kinetics based on the information of in vitro release.

(d) Correlation of t^* and $(M_r/M_0)^*$ with A/C_s—As aforementioned, the fraction of a solute remaining in the matrix at t^* can be noticeable at small A/C_s. Figure 11 illustrates the remaining fraction at t^*, $(M_r/M_0)^*$, as a function of A/C_s for three geometries, where M_r and M_0 denote the remaining and the initial amount of the solute in the matrix, respectively. $(M_r/M_0)^*$ drops drastically as A/C_s increases from 1 to 2 and then decreases gradually till $A/C_s = 5$,

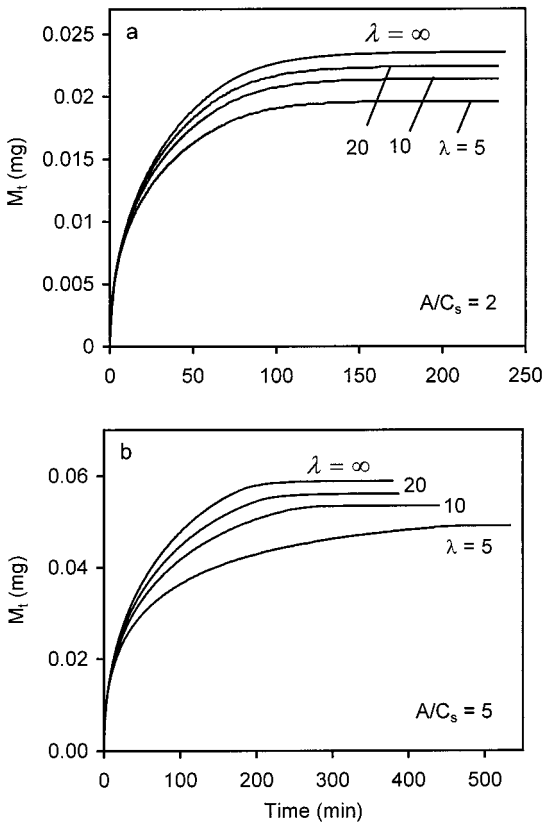

Figure 10—Influence of effective volume ratio on the amount of solute released from a cylinder ($L = 0.1$ cm, $D_1 = 1 \times 10^{-6}$ cm^2/s, $K = 1$). (a) $A/C_s = 2$ and (b) $A/C_s = 5$. The 100% solute released is indicated by the plateau of the release curve for $\lambda = \infty$.

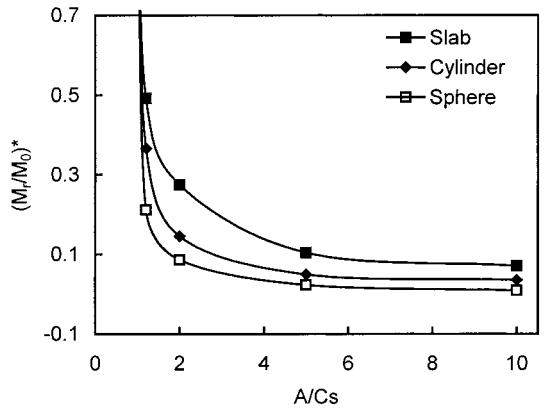

Figure 11—The fraction of a solute remaining in the matrix at t^* for three geometries in a perfect sink ($L = 0.1$ cm, $D_1 = 1 \times 10^{-6}$ cm^2/s).

beyond which the reduction in $(M_r/M_0)^*$ becomes insignificant. The remaining fraction of the solute is the largest for the slab and the smallest for the sphere, suggesting that $(M_r/M_0)^*$ is a function of diffusion rate. One may infer that the remainder could increase as the diffusion coefficient, or the external volume decreases because of the reduced release rate. $(M_r/M_0)^*$ can be correlated with A/C_s by

$$(M_r/M_0)^* = B[A/C_s]^{-\alpha} \qquad (11)$$

where B and α are constants. The values of B and α for three basic geometries were obtained from the nonlinear regression of the data in Figure 11 and are listed in Table 1.

A good linear relationship between the t^* and A/C_s is revealed by Figure 12 for all three geometries. Table 1 summarizes the slope (β) and intercept (γ) of the linear function (eq 12) together with the correlation coefficients of the linear regression.

Table 1—Parameters in Eqs 11 and 12 Evaluated from the Data in Figures 11 and 12 for Three Basic Geometries in a Perfect Sink

geometry	β (slope)	γ (intercept)	r^2 (correlation coefficient)	B	α
slab	75.57	58.69	0.9986	0.7098	1.086
cylinder	36.76	23.72	0.9949	0.5696	1.348
sphere	25.34	14.60	0.9951	0.4678	1.810

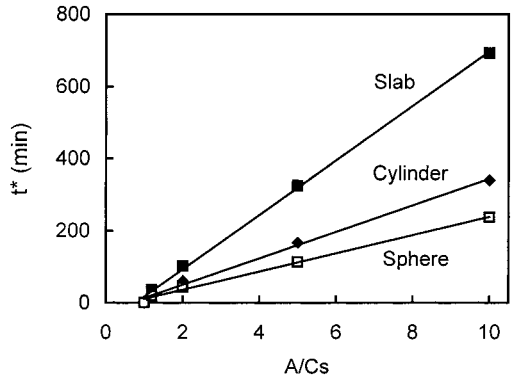

Figure 12—Dependence of t^* on A/C_s for three geometries in a perfect sink ($L = 0.1$ cm, $D_1 = 1 \times 10^{-6}$ cm^2/s).

$$t^* = \beta[A/C_s] - \gamma \qquad (12)$$

Again, the influence of A/C_s on t^* is the greatest for the slab and the least for the sphere, suggesting that, like $(M_r/M_0)^*$, t^* is also dependent on the diffusion rate.

(e) Boundary Layer Effect—It has been demonstrated that the stagnant boundary layer is responsible for the reduced release rate.[2,13] It was intended here to develop a model with consideration of the effect of boundary layer rather than elaborating its mechanism. From the simulation point of view, the boundary layer acts as a thin layer coating. Hence, a thin layer element with corresponding material properties was introduced to the surface of the matrix of interest. The computed release profile was compared with the theoretical solution reported by Roseman and Higuchi[2] for a cylinder in a sink. As depicted in Figure 13a, the finite element solution matches the analytical solution well for a solute with diffusion coefficients in the matrix and in the boundary layer, $D_1 = 1 \times 10^{-6}$ cm^2/s, and $D_2 = 5 \times 10^{-6}$ cm^2/s, respectively, and the thickness of the boundary layer, $h_a = 0.01$ cm. Figure 13b shows that the release rates of a solute from three basic geometries ($L = 0.1$ cm, $A/C_s = 5$) into a finite volume of liquid ($V/V_1 = 10$, $K = 2$) is reduced in the presence of a boundary layer of thickness, $h_a = 0.01$ cm, i.e., $h_a/L = 0.1$. This trend agrees with general observations. The degree of the reduction for the cylinder is slightly greater than the prediction by Roseman & Higuchi's model.[2] For example, at $t = 100$ min, the reduction in the fractional release calculated in this work is ~4% in the presence of a boundary layer, whereas it is ~1% by their model for the same cylinder in a perfect sink. This is likely a result of the difference in the volume of surrounding medium, which is infinite in the analytical solutions and is finite ($V/V_1 = 10$) in the numerical solutions. In a finite volume of liquid, the drug concentration builds up, contributing to a slower release rate and a greater boundary-layer effect.

It is interesting to notice a geometry dependence of the boundary-layer effect. The effect appears the most marked

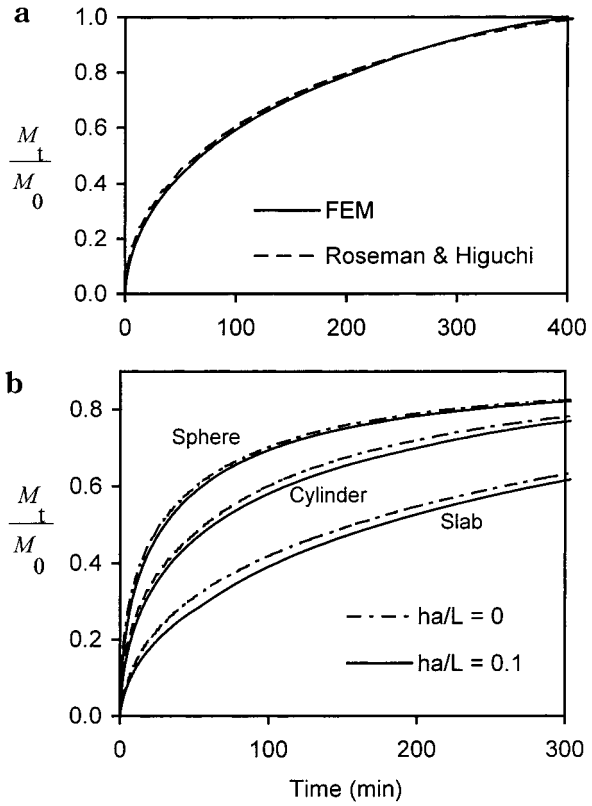

Figure 13—(a) Fractional release of a dispersed solute from a cylinder into a perfect sink with boundary layer resistance ($A/C_s = 10$, $L = 0.1$ cm, $h_a/L = 0.1$, $D_1 = 1 \times 10^{-6}$ cm^2/s, $D_2 = 5 \times 10^{-6}$ cm^2/s, $K = 2$). Comparison of FE solution with the solution from Roseman and Higuchi with pseudo-steady-state assumption.[2] (b) Effect of boundary layer resistance on the release rate of a solute from three geometries in a well-stirred liquid of finite volume ($\lambda = 10$, $A/C_s = 5$, $L = 0.1$ cm, $D_1 = 1 \times 10^{-6}$ cm^2/s, $D_2 = 5 \times 10^{-6}$ cm^2/s, $K = 2$).

for the slab and the least for the sphere. For example, at $t = 100$ min, the reduction in the fractional release in the presence of a boundary layer is 7.2%, 4.1%, and 1.2% for the slab, cylinder, and sphere, respectively. This suggests that the boundary layer effect depends on the relative release rate in the matrix to that in the boundary layer. The solute release from the slab is the slowest and thus is affected most by the boundary layer.

Multidimensional-Release Convex Tablets—The finite element method presented here can model complex matrix dosage forms of virtually any shape. However, the emphasis was placed on matrix tablets here in the hope that the efforts of this work could facilitate the design of this popular controlled-release dosage form for oral administration. For convex tablets with three-dimensional release, dispersed initial drug loading, and the boundary layer resistance, no analytical solution has been reported. This original work provides insight into the release kinetics in relation to design parameters such as A/C_s ratio and environmental conditions. The fractional release, M_t/M_∞, of a drug from convex tablets with different A/C_s ratios into a well-mixed finite volume is depicted in Figure 14, where M_∞ is the amount of drug released at the final stage, $V/V_1 = 10$, $K = 1$, and $D_1 = 1 \times 10^{-6}$ cm^2/s. Clearly, the time for the completion of the release increases with increasing A/C_s ratio, which is consistent with the observation of other geometries.

Figure 15 shows the moving boundary and concentration distribution within a tablet with $A/C_s = 2$ in a well-mixed finite volume ($V/V_1 = 10$, $K = 1$, and $D_1 = 2 \times 10^{-7}$ cm^2/s). The concentration profiles are similar to those in the slab. However, unlike the release into a perfect sink (Figures 3,

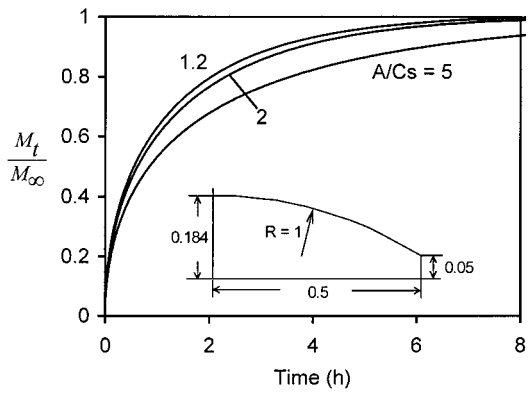

Figure 14—Fractional release of a dispersed drug from a convex tablet with $A/C_s = 1.2$, 2, and 5 into a well-mixed finite volume ($\lambda = 10$, $D_1 = 1 \times 10^{-6}$ cm^2/s, $K = 1$).

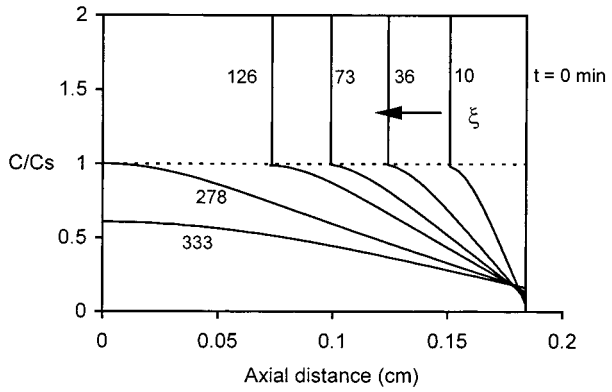

Figure 15—Moving boundary and concentration profile of a dispersed drug for a convex tablet in a well-stirred liquid of finite volume ($\lambda = 10$, $D_1 = 2 \times 10^{-7}$ cm^2/s, $K = 1$).

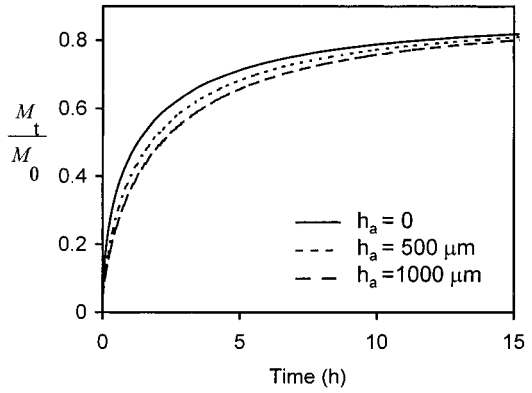

Figure 16—Influence of boundary layer resistance on the fractional release of a dispersed drug from convex tablets into a well-stirred finite volume ($A/C_s = 5$, $\lambda = 10$, $D_1 = 1 \times 10^{-6}$ cm^2/s, $D_2 = 5 \times 10^{-6}$ cm^2/s, $K = 2$).

6, and 9), the concentration near the surface of the tablet increases with time, reflecting concentration build-up in the bulk solution of a limited volume. Such concentration build-up leads to a smaller driving force for diffusion, i.e., the concentration gradient between the matrix and the medium, and thus lower release rate. This result explains partly why the in vivo release is slower than the in vitro one.

Another factor that is often associated with the lower in vivo release rate is the diffusion boundary layer. The boundary-layer effect on the fractional release, M_t/M_0, where M_0 is the initial amount of the solute, is illustrated in Figure 16 for a tablet with $A/C_s = 5$ in a well-mixed finite volume ($V/V_1 = 10$, $K = 2$, $D_1 = 1 \times 10^{-6}$ cm^2/s, and $D_2 = 5 \times 10^{-6}$ cm^2/s). As shown by the figure, the release rate

decreases as the boundary-layer thickness increases. It should be indicated that the curves in Figure 16 could only reach ~83% of the initial loading at a much longer time, e.g., 25 h, as a result of saturation of the medium.

In reality, polymeric matrix tablets involve not only the moving boundary of a dispersed drug, but also the moving boundaries of swelling and erosion. The finite element model for matrix tablets with swelling and erosion has been developed by our group for $A/C_s \leq 1$.[22] Further work on incorporation of all three moving boundaries into the model is in progress.

Conclusions

The numerical solutions of differential equations have been obtained by the finite element method for diffusional release of a dispersed solute from slab, sphere, cylinder, and convex tablet into various external volumes. The kinetics of the entire release process have been presented for these matrixes with a broad range of A/C_s ratios and boundary conditions varying from a perfect sink to a finite volume with boundary-layer resistance. The evolution of solute concentration profiles in the matrixes has been revealed. The shape of the concentration profiles depends on the geometry of the matrixes. The nonlinearity of the profiles is found to be sphere > cylinder > slab, in the same order of the release rate. The numerical results for the sink conditions agree well with the existing analytical solutions. The existence of boundary-layer resistance reduces the release rate, and the degree of the reduction increases with increasing thickness.

References and Notes

1. Higuchi, T. Rate of Release of Medicaments from Ointment Bases Containing Drugs in Suspension. *J. Pharm. Sci.* **1961**, *50*, 874−875.
2. Roseman, T. J.; Higuchi, W. I. Release of Medroxyprogesterone Acetate from a Silicone Polymer. *J. Pharm. Sci.* **1970**, *59*, 353−357.
3. Paul, D. R.; McSpadden, S. K. Diffusional Release of a Solute from a Polymer Matrix. *J. Membr. Sci.* **1976**, *1*, 33−48.
4. Lee, P. I. Diffusional Release of a Solute from a Polymeric Matrix-Approximate Analytical Solutions. *J. Membr. Sci.* **1980**, *7*, 255−275.
5. Baker, R. W.; Lonsdale, H. K. Controlled Release: Mechanisms and Rates, In *Controlled Release of Biologically Active Agents*; Tanquary, A. C., Lacey, R. E., Eds.; Plenum Press: New York, 1974, pp 15−71.
6. Cobby, J.; Mayersohn, M.; Walker, G. C. Influence of shape Factors on Kinetics of Drug Release from Matrix Tablets. I: Theoretical, *J. Pharm. Sci.* **1974**, *63*, 725−732.
7. Rhine, W. D.; Hsieh, D. S. T.; Langer, R. Polymers for Sustained Macromolecule Release: Procedures to Fabricate Reproducible Delivery systems and Control Release Kinetics, *J. Pharm. Sci.* **1980**, *69*, 265−270.
8. Rhine, W. D.; Sukhatme, V.; Hsieh, D. S. T.; Langer, R. A New Approach to Achieve Zero-Order Release Kinetics from Diffusion-Controlled Polymer Matrix Systems,. In *Controlled Release of bioactive Materials*; Baker, R., Ed.; Academic Press: New York, 1980; pp 177−187.
9. Brooke, D.; Washkuhn, R. J. Zero-Order Drug Delivery System: Theory and Preliminary Testing, *J. Pharm. Sci.* **1977**, *66*, 159−162.
10. Kuu, W. Y.; Yalkowsar, S. H. Multiple-Hole Approach to Zero-Order Release. *J. Pharm. Sci.* **1985**, *74*, 926−933.
11. Tojo, K. Intrinsic Release Rate from Matrix-Type Drug Delivery Systems, *J. Pharm. Sci.* **1985**, *74*, 685−687.
12. Gupta, D. V. S.; Sparks, R. E. Mathematical Model for Progesterone Release from injectible Poly(Lactic Acid) Microcapsules in vitro. In *controlled Release of Bioactive Materials*; Backer, R., Ed.; Academic Press: New York, 1980; pp 198−212.
13. Ayres, J. W.; Lindstrom, F. T. Diffusion Model for Drug Release from Suspensions. I: Theoretical considerations. *J. Pharm. Sci.* **1977**, *66*, 654−662.
14. Lindstrom, F. T.; Ayres, J. W. Diffusion Model for Drug Release from Suspensions. II: Release to a Perfect Sink. *J. Pharm. Sci.* **1977**, *66*, 662−668.
15. Chandrasekaran, S.; Paul, D. R. Dissolution-Controlled Transport from Dispersed Matrixes. *J. Pharm. Sci.* **1982**, *71*, 1399−1402.
16. Fan, L. T.; Singh, S. K. Controlled Release: A Quantitative Treatment, Springer-Verlag: New York, 1989.
17. Abdekhodaie, M. J.; Cheng, Y.-L. Diffusional Release of a Dispersed Solute From Planar and Spherical Matrixes Into Finite External Volume.. *J. Controlled Relat.* **1997**, *43*, 175−182.
18. Chien, Y. W. Thermodynamics of Controlled Drug Release from Polymeric Delivery Devices. In *Controlled Release Polymeric Formulations*; Paul, D. R., Harris, F. W., Eds.; ACS Symposium Series 33, 1976; pp 53−71.
19. Zhou, Y.; Wu, X. Y. Finite Element Analysis of Diffusional Drug Release from Complex Matrix Systems. I. Complex geometries and composite structures. *J. Controlled Release* **1997**, *49*, 277−288.
20. Wu, X. Y.; Zhou, Y. Finite Element Analysis of Diffusional Drug Release from Complex Matrix Systems. II. Factors Influencing Release Kinetics, *J. Controlled Release* **1998**, *51*, 57−72.
21. Wu, X. Y.; Eshun, G.; Zhou, Y. Effect of Interparticulate Interaction on Kinetics of Drug Release in Microsphere Ensembles. *J. Pharm. Sci.* **1998**, *87*, 586−593.
22. Wu, X. Y.; Zhou, Y. Numerical Analysis of Drug Release from Matrix Tablets with Moving Boundaries. *Proc. Intern. Symp. Controlled Release Bioact. Mater.* **1998**, *25*, 451−452.
23. Crank, J. *The Mathematics of Diffusion*; Oxford University Press: London, 1975.

JS9804361